

Preparation and Characterization of Phase-Segregated Vesicles of Photopolymerizable Diacetylene Mixed with Nonpolymerizable Amphiphiles

Jin Matsumoto,* Koshiro Yoneda, Jun Tasaka, Tsutomu Shiragami, and Masahide Yasuda

Department of Applied Chemistry, Faculty of Engineering, University of Miyazaki,
Gakuen-Kibanadai, Miyazaki 889-2192

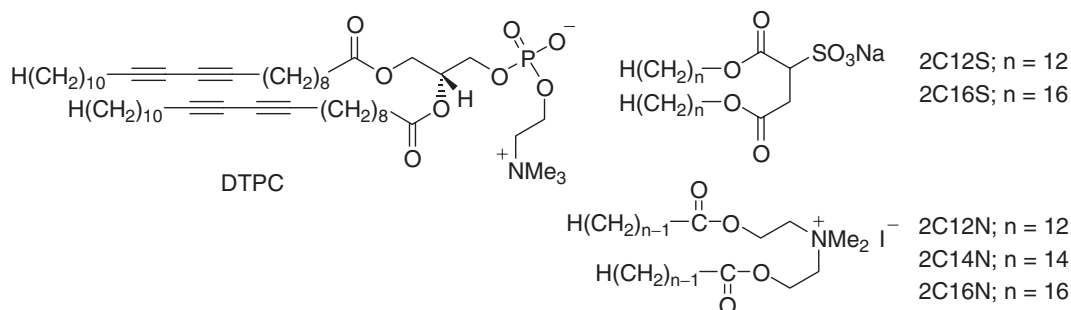
Received July 9, 2010; E-mail: jmatsumo@cc.miyazaki-u.ac.jp

A mixture of sodium 1,2-di(hexadecyloxycarbonyl)ethanesulfonate (2C16S) with photopolymerizable 1,2-di(10,12-tricosadiynoyl)-*sn*-glycerol 3-phosphocholine (DTPC) in a 2:100 ratio was treated by modified thin-film hydration to give an aggregate which became polymerized giant vesicles (GVs) under irradiation at 254 nm. The autofluorescence of the GV was analyzed with a confocal laser scanning microscope at the cross section, revealing a 3.8- μm diameter ring shape and the presence of a dark part of ca. 1 μm in the ring. When octadecylrhodamine B (RhB) as an amphiphilic fluorescence probe was added to the GV, the fluorescence of RhB was emitted from the whole ring. Therefore, phase segregation of 2C16S from DTPC was confirmed. Similarly, mixed vesicles of *N,N*-di(2-hexadecanoyloxyethyl)dimethylammonium iodide with DTPC were found to be 3.7- μm diameter phase-segregated vesicles with a dark portion of ca. 1 μm on the ring in the cross sectional image. On the other hand, DTPC vesicles mixed with 1,2-di(dodecyloxycarbonyl)ethanesulfonate, *N,N*-di(2-dodecanoyloxyethyl)dimethylammonium iodide, and *N,N*-di(2-tetradecanoyloxyethyl)dimethylammonium iodide formed sphere structures filling the inside of the vesicles. The segregation mechanism was explained by the difference in the main phase transition temperature of each amphiphile.

Lipids or amphiphilic compounds can form highly ordered aggregates with unique shapes and functions by self-assembly in aqueous solution.^{1,2} A vesicle, which is an egg-shaped lipid aggregate (liposome), is a typical lipid assembly. A variety of vesicles of natural lipids or synthetic-amphiphilic compounds have been characterized from the standpoints of the mimicking of biomembranes and the development of liposome drugs such as for gene delivery and cancer therapy.³ Their performance has been modified by the following methods. The control of stability and release of drug has been modified by polymerization of vesicles using photopolymerizable diacetylenic amphiphiles which can form self-assembled structures in aqueous solution.^{4,5} The resulting polydiacetylene has been applied as a carrier of drugs^{6–8} and various colorimetric biosensors.^{9,10} Moreover, the combination of the liposome and the additional components modified the surface properties

of liposome such as charge or specific binding using self-assembly and chemical transformation.^{3,11}

Among the modification of functionalized vesicles, the phase segregation of vesicles has received much attention in order to elucidate the functions of signal transduction and membrane transport of the vesicles.¹² Phase segregation of vesicles has been usually examined by calorimetric analysis and fluorescence microscopy using phase-selective fluorescence probes.¹³ Diacetylenic phosphatidylcholine, 1,2-di(10,12-tricosadiynoyl)-*sn*-glycerol 3-phosphocholine (DTPC), is known to have high affinity for a variety of lipid molecules because DTPC contains the hydrophilic head group occurring in natural phospholipids (Scheme 1).^{7,14–16} Okazaki and co-workers have prepared substrate-supported planar lipid bilayers composed of polymeric DTPC and fluid-nonpolymerizable phospholipids under lithographically controlled UV irradiation



Scheme 1. The polymerizable DTPC, anionic 2C n S, and cationic 2C n N amphiphiles.

tion.¹⁷ The bilayers obtained were characterized by atomic force microscopy, fluorescence microscopy, and ellipsometry. On the other hand, photopolymerized DTPC molecules emit autofluorescence at 550 nm,^{18,19} similar to other diacetylenic compounds. The autofluorescence of polydiacetylene is useful to distinguish it from nonpolymerizable amphiphiles in fluorescence microscopy without addition of any fluorescence probes. Therefore, our attention was focused on the preparation of phase-segregated vesicles between nonpolymerizable amphiphiles and polymerizable DTPC which are large enough to analyze with a confocal laser scanning fluorescence microscope (CLSM). Here, it will be examined whether the small amount of nonpolymerizable amphiphiles could change the phase segregation and the morphology of the mixed vesicles by changing the alkyl-chain length of the nonpolymerizable amphiphiles.

Experimental

Materials. Water was purified by a Millipore Elix III (USA). Glassware, such as flasks and glass plates, was washed with concentrated nitric acid at 90 °C for 2 h and rinsed with pure water for use in the preparation and observation of vesicle solutions. The washed glassware was immersed in an aqueous KOH solution (1 mol dm⁻³) for 12 h, followed by sonication in pure water. The cleaned glassware was stored in pure water.

The DTPC was purchased from Avanti Polar Lipids, Inc. (USA) and was used without further purification. As a lipophilic fluorescence probe, octadecylrhodamine B (RhB, emission maximum at 585 nm) was purchased from Invitrogen (USA). 2-[4-(2-Hydroxyethyl)-1-piperazinyl]ethanesulfonic acid (0.01 mol dm⁻³, HEPES, Dojindo, Japan) was dissolved in pure water and pH was adjusted to 7.0 with aqueous NaOH solution. The resulting HEPES buffer solution was filtered through a 1 µm pore size membrane and bubbled with argon gas before use.

Instruments. ¹H NMR (400 MHz) and ¹³C NMR (100 MHz) spectra were taken on a Bruker AV 400M spectrometer (Germany) for CDCl₃ and CD₃OD solutions using SiMe₄ as an internal standard. Matrix-assisted laser desorption/ionization mass spectra (MALDI-MS) were measured on a Bruker Daltonics Autoflex III TOF/TOF (Germany) in the positive ion mode. Calibration of the mass number was performed with an internal standard using poly(ethylene glycol). UV-vis spectra of the solutions were obtained with a JASCO V-550 spectrophotometer (Japan). Fluorescence spectra were measured on a Shimadzu FR-5300PC fluorometer (Japan).

General Procedure for the Synthesis of Anionic Amphiphiles (2CnS). Double-chain anionic amphiphiles without the polymerizable group, sodium 1,2-di(alkyloxycarbonyl)ethanesulfonate (2CnS; *n* = 12, alkyl = dodecyl and *n* = 16, alkyl = hexadecyl), were synthesized according to the literature.²⁰ 1-Alkanol (3.3 mmol) was refluxed with maleic anhydride (1.5 mmol) in the presence of concentrated sulfuric acid (0.10 cm³) in toluene (50 cm³) at 110 °C in a Dean-Stark apparatus. After the neutralization with aqueous NaHCO₃ solution, the crude dialkyl maleate was extracted with toluene and purified by recrystallization from hexane. The dialkyl maleate (1 mmol) was refluxed in an aqueous solution (100 cm³) of NaHSO₃ (35 g) for 3 h under bubbling with air. After neutralization with NaHCO₃ and evaporation, the result-

ing residue was dissolved in hot methanol and filtered. After evaporation of the filtrate, the crude product was washed with hexane and water and purified by recrystallization from hexane. The identification was performed by the comparison of spectral data with authentic samples.²⁰

General Procedure for the Synthesis of Cationic Amphiphiles (2CnN). The esterification of *N*-methyldiethanolamine was performed by the reaction of *N*-methyldiethanolamine (5 mmol) and fatty acid (10.6 mmol) in the presence of 4-dimethylaminopyridine (3.2 mmol) and *N,N'*-dicyclohexylcarbodiimide (10.6 mmol) in CHCl₃ (30 cm³). The mixture was cooled in an ice-water bath for 1 h and then stirred at room temperature for 1 week. After filtration to remove precipitated 1,3-dicyclohexylurea, the solution was washed with HCl (0.01 mol dm⁻³) and a saturated aqueous NaCl solution, and then dried with Na₂SO₄. The solution was evaporated to yield crude *N,N*-di(2-alkanoyloxyethyl)methylamine, which was subjected to purification by column chromatography. The quaternization of *N,N*-di(2-alkanoyloxyethyl)methylamine (1 mmol) by methyl iodide (50 mmol) was performed in dry MeCN (10 cm³). After stirring for 1 h under a nitrogen atmosphere, the mixture was evaporated to yield a crude product which was purified by recrystallization from methanol.

***N,N*-Di(2-dodecanoyloxyethyl)dimethylammonium Iodide (2C12N):** ¹H NMR: δ 0.88 (t, *J* = 7.0 Hz, 6H), 1.26–1.30 (m, 32H), 1.62 (quint, *J* = 7.7 Hz, 4H), 2.38 (t, *J* = 7.7 Hz, 4H), 3.56 (s, 6H), 4.16–4.18 (m, 4H), 4.60–4.62 (m, 4H). ¹³C NMR: δ 14.08, 22.65, 24.63, 29.10, 29.25, 29.31, 29.45, 29.58, 26.58, 31.87, 34.07, 52.93, 57.41, 64.01, 172.71; Exact MS (MALDI-MS) Calcd for C₃₀H₆₀NO₄: 498.4522, Found 498.4506.

***N,N*-Di(2-tetradecanoyloxyethyl)dimethylammonium Iodide (2C14N):** ¹H NMR: δ 0.88 (t, *J* = 6.8 Hz, 6H), 1.26–1.33 (m, 40H), 1.58–1.65 (m, 4H), 2.38 (t, *J* = 7.7 Hz, 4H), 3.57 (s, 6H), 4.15–4.18 (m, 4H), 4.60–4.62 (m, 4H). ¹³C NMR: δ 14.08, 22.66, 24.64, 29.11, 29.26, 29.33, 29.47, 29.60, 29.63, 29.63, 29.67, 31.89, 34.07, 52.94, 57.42, 64.02, 172.71; Exact MS (MALDI-MS) Calcd for C₃₄H₆₈NO₄: 554.5148, Found 554.5163.

***N,N*-Di(2-hexadecanoyloxyethyl)dimethylammonium Iodide (2C16N):** ¹H NMR: δ 0.88 (t, *J* = 7.0 Hz, 6H), 1.26–1.30 (m, 48H), 1.62 (quint, *J* = 7.8 Hz, 4H), 2.38 (t, *J* = 7.8 Hz, 4H), 3.57 (s, 6H), 4.16–4.18 (m, 4H), 4.60–4.62 (m, 4H). ¹³C NMR: δ 14.08, 22.66, 24.64, 29.11, 29.26, 29.34, 29.48, 29.61, 29.64, 29.65, 29.65, 29.65, 29.65, 31.90, 34.07, 52.92, 57.40, 64.01, 172.71; Exact MS (MALDI-MS) Calcd for C₃₈H₇₆NO₄: 610.5774, Found 610.5782.

Fluorescence Imaging. The CLSM analysis was performed with an Olympus FV-300 (confocal aperture: 150 µm, Japan) equipped with an objective lens (×100 oil, numerical aperture: 1.3). A vesicle solution was placed in the hole of a silicon spacer (1 cm × 1 cm, 50-µm thickness) on a slide glass and was enclosed with a cover glass. The objective lens was moved downward to obtain cross-sectional images of the vesicles. The moving distance (*z*) was defined as the distance from the uppermost surface of the vesicle (*z* = 0). The CLSM had a positional resolution of ±0.1 µm in the vertical direction and ±0.1 µm in the horizontal direction. Fluorescence images of the polymerized DTPC were measured by passing through

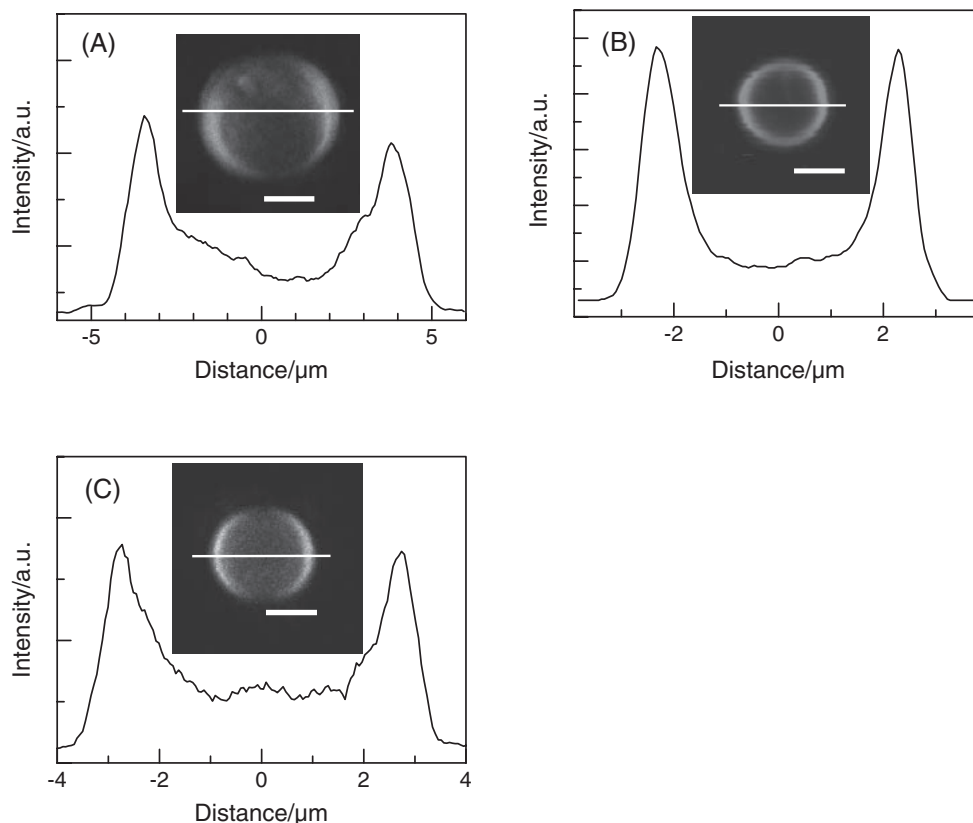


Figure 1. Distribution of the fluorescence intensity ($>565 \text{ nm}$) along a line on cross-sectional CLSM images (inset) of **1** at $z = 3.6 \mu\text{m}$ (A) and **3** at $z = 2.3 \mu\text{m}$ under 543-nm laser excitation (B); and **3'** at $z = 2.8 \mu\text{m}$ under 488-nm laser excitation (C). The scale bar in inset is in 3 μm units.

cutoff filter ($>565 \text{ nm}$) under the excitation by 488-nm laser irradiation. The nonirradiated DTPC vesicles and nonpolymerizable amphiphiles vesicles were observed using the addition of 1 mol % RhB relative to the amount of the amphiphiles under 543-nm laser irradiation.

Measurement of Phase Transition Temperatures of 2C n N. Differential scanning calorimetric (DSC) measurements were carried out with a Rigaku Thermo Plus 8240 differential scanning calorimeter (Japan). Vesicle solution was prepared by TFH (described below) of 2C n N ($1.67 \mu\text{mol cm}^{-3}$). Vesicles were concentrated by centrifugation of the solution and the removal of supernatant. The collected vesicle solution was resuspended in water to give a solution ($10 \mu\text{mol cm}^{-3}$). The vesicle solution ($10 \times 10^{-6} \text{ dm}^3$) was placed in a hermetically sealed aluminum pan. DSC measurement was performed at a heating rate of 2°C min^{-1} .

Results and Discussion

Preparation of Vesicles by Thin-Film Hydration. Our first effort was paid to prepare vesicles of a large enough size to analyze by CLSM. It has been reported that sodium 1,2-di(dodecyloxycarbonyl)ethanesulfonate (2C12S) treated by the usual direct sonication method, forms vesicles at submicrometer scale which is too small to be analyzed by optical microscopy.²⁰ Therefore, we performed the preparation of micrometer size vesicles of 2C12S by modified thin-film hydration (TFH) as follows. The 2C12S was dissolved in $\text{CHCl}_3\text{-MeOH}$ (10:1) to give a $1.0 \times 10^{-4} \text{ mol dm}^{-3}$ solution.

The solvents were evaporated gently to produce a thin film. After the thin film was dried under a vacuum at 75°C for 3 h, the dried film was hydrated in HEPES buffer solution at 80°C under sonication. The solution was left to stand at 22.5°C for 3 days during the formation of an aggregate. After RhB acting as fluorophore was added to the aggregates, the fluorescence image coming from RhB was analyzed on the CLSM (Figure 1A). A vesicle structure with a ring-shaped image and a dark area inside the ring were observed at every cross section of the selected aggregate. When the fluorescence intensities were mapped in the cross section at a $3.6 \mu\text{m}$ depth (z) from the uppermost of the aggregate, two intensity maxima appeared $7.1 \mu\text{m}$ apart from each other which was defined as the diameter of the vesicle. So we called it a giant vesicle (GV) of 2C12S (**1**). The TFH method was successfully applied to sodium 1,2-di(hexadecyloxycarbonyl)ethanesulfonate (2C16S) which formed the GV of 2C16S (**2**) with a $3.4 \mu\text{m}$ diameter. The peak width at the half height of fluorescence intensity was about $0.5 \mu\text{m}$. This size was not comparable to the molecular size of the bilayer of 2C n S, because the resolution limit of the fluorescence microscopy was near $0.5 \mu\text{m}$.

In general, DTPC forms aggregated structures with supramolecular morphologies such as vesicles¹⁵ and helical or tubular structures in aqueous solution,^{21,22} depending on the preparation conditions. Here, the TFH of DTPC was proceeded, giving GV **3** whose diameter was determined to be $4.5 \mu\text{m}$ by CLSM analysis using RhB (Figure 1B). It is well known that a diacetylene moiety of DTPC was photopolymerized topotacti-

cally to give the ene-yne backbone. Therefore, the solution of **3** was irradiated at 254 nm for 60 min at 4 °C to give the polymerized GV **3'**. The diameter of **3'** was measured to be 5.5 μm from autofluorescence images (Figure 1C). Thus, single GVs **1**, **2**, **3**, and **3'** were successfully prepared from 2C12S, 2C16S, and DTPC by TFH, respectively (Table 1).

Mixed Vesicles of DTPC with 2C n S. The mixed vesicles of DTPC were prepared by mixing 2C16S with DTPC in a molar ratio of 2:100 followed by TFH. Aqueous solution of the resulting mixed aggregates was immediately irradiated at 254 nm for 60 min to give the polymerized aggregate **4**. The fluorescence intensity of the selected **4** was analyzed at the cross section $z = 2.0 \mu\text{m}$, revealing the 3.8- μm diameter ring shape and the presence of a dark part of ca. 1 μm in the ring (Figure 2A). When RhB was added to **4**, fluorescence of RhB appeared in the whole ring of **4**, but no fluorescence came from inside of GV. Therefore, the dark part on the ring was composed of 2C16S. Thus, the formation of the phase-segregated GV (s-GV) between 2C16S and DTPC was proven. A similar treatment was applied to a mixture 2C12S with DTPC. However, the resulting aggregate **5** showed almost uniform fluorescence coming from the whole circular plane

with a diameter of 4.0 μm , revealing that **5** was not a vesicle structure but a filled sphere (Figure 2B).

Mixed Vesicles of DTPC with 2C n N. It is expected that DTPC forms the mixed vesicles with not only the anionic 2C n S but also the cationic surfactants, since DTPC is a zwitterion. As cationic surfactants therefore, *N,N*-di(2-alkanoyloxyethyl)dimethylammonium iodide (2C n N: $n = 12$ (dodecanoyl), $n = 14$ (tetradecanoyl), and $n = 16$ (hexadecanoyl); Scheme 1) were prepared. The molar ratio of 2C n N and DTPC was optimized to be 2:100, judging from F values in UV-spectra described below (Figure S1 in Supporting Information). The mixture of 2C16N and DTPC in a molar ratio of 2:100 was subjected to TFH and UV irradiation for 60 min to give aggregate **6**. The selected **6** was analyzed by the fluorescence intensity at cross sections (Figure 3A). The diameter of the ring was measured to be 3.7 μm and a dark part 1 μm in length was observed in the cross section in the range of $z = 1.4$ – $2.6 \mu\text{m}$. Detailed images in the cross section are shown in the Supporting Information Figure S2. When RhB was added to **6**, the emission was coming from the whole ring. Therefore, the dark part was composed of 2C16N. Based on the observed diameter (3.7 μm), the surface area of the nonfluorescent 2C16N part and the polymerized DTPC part of **6** were calculated to be 0.79 and 43 μm^2 , respectively. The surface ratio of 2C16N and DTPC was 1.8:100, a ratio which is in good agreement with the mixing ratio of 2C16N and DTPC (2:100) in the preparation. Therefore, DTPC and 2C16N were completely segregated into two phases to give s-GV.

It was confirmed that the TFH treatment of 2C14N and 2C12N gave single GVs of 4.6 and 10.6 μm diameters, respectively (See Supporting Information Figure S3). A mixed solution of 2C12N or 2C14N and DTPC at a molar ratio of 2:100 was treated by TFH and polymerized by UV irradiation. However, the fluorescence from DTPC was emitted from the whole circular plane at all z positions, resulting in the filled aggregates **7** and **8** (Figure 3B and Figures S4 and S5 in Supporting Information).

Structures of the Polymerized DTPC in Vesicles. It is known that DTPC is polymerized in the solid phase, depending on the vesicle structure.²³ The color changes of polydiacetylene are attributed to the length of the overlapping π -orbitals which can be affected by conformational change in the polymer backbone.²⁴ In the absorption spectra of **3'**, the absorption

Table 1. The Characterization of Single Vesicles **1**–**3** and Mixed Vesicles **4**–**8**

Aggregates	Main amphiphile	Other amphiphile	Diameter ^{a)} / μm	Structure ^{b)}	F / $\%$ ^{c)}
1	2C12S	—	7.1	GV	—
2	2C16S	—	3.4	GV	—
3	DTPC	—	4.5	GV	—
3' ^{d)}	DTPC	—	5.5	GV	24
4 ^{d)}	DTPC	2C16S	3.8 (1.0) ^{e)}	s-GV	26
5 ^{d)}	DTPC	2C12S	4.0	filled	17
6 ^{d)}	DTPC	2C16N	3.7 (1.0) ^{e)}	s-GV	25
7 ^{d)}	DTPC	2C14N	7.5	filled	13
8 ^{d)}	DTPC	2C12N	9.0	filled	16

a) Diameter was measured from the intensity maxima at the cross section of the aggregate. b) The structure of the aggregates: GV: giant vesicle, s-GV: phase-segregated GV, filled: aggregate filled inside. c) F values after 60-min irradiation. d) Photopolymerized vesicles. e) The values of parenthesis are a length of the dark region in μm on the ring.

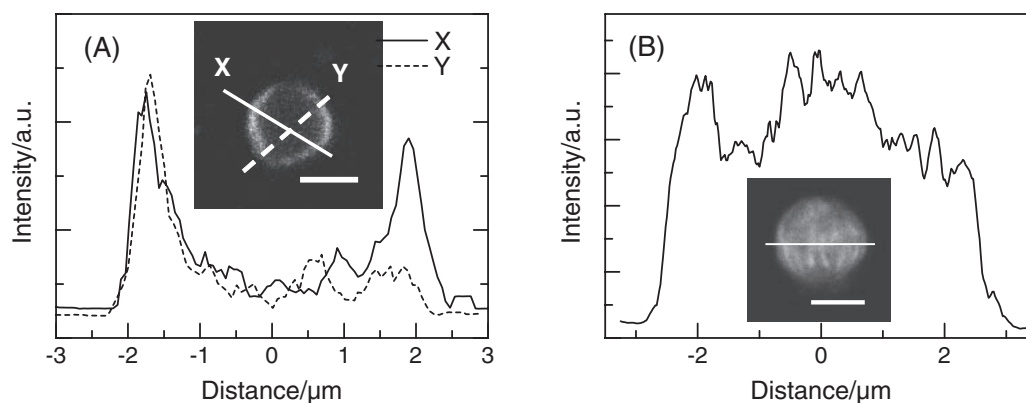


Figure 2. Distribution of the fluorescence intensity ($>565 \text{ nm}$) along a line on cross-sectional CLSM images (inset) of **4** at $z = 2.0 \mu\text{m}$ (A) and **5** at $z = 2.2 \mu\text{m}$ (B) under 488-nm laser excitation. The scale bar in inset is in 3 μm units.

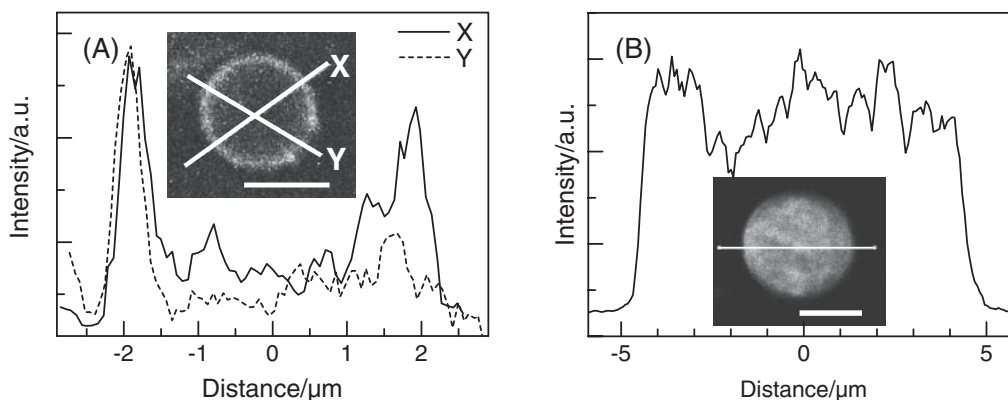


Figure 3. Distribution of the fluorescence intensity (>565 nm) along a line on cross-sectional CLSM images (inset) of **6** at $z = 2.2$ μm (A) and **8** at $z = 4.5$ μm (B) under 488-nm laser excitation. The scale bar is in 3 μm units.

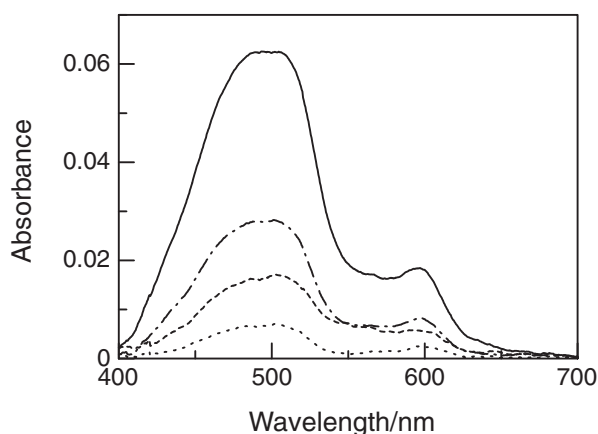


Figure 4. Absorption spectral change of the solution of DTPC under UV irradiation for 5 (dotted line), 15 (broken line), 30 (dashed line), and 60 min (solid line).

maxima at 600 and 485 nm are assigned to be long and short conjugation lengths, respectively (Figure 4).^{25–27} Therefore, the polymerization behavior can be evaluated by absorption spectra of the polymerized DTPC. The contribution of a long conjugation length to short conjugation length was evaluated by the ratio (F) of absorbance at 600 nm (A_{600}) to that at 485 nm (A_{485}): F (%) = $100 \times A_{600}/A_{485}$. The F value of **3'** was determined to be 24% in a steady state, as shown in time-course plots of the F values (Figure 5A). The F values of s-GV **4** and **6** were 26% and 25%, which are similar to that of **3'**. On the other hand, the F values of the mixed vesicles of **5**, **7**, and **8** were 17%, 17%, and 13%, respectively, under UV irradiation for 60 min, although the F values at the beginning of the UV irradiation were higher than 20% (Figure 5B).

The additive effects of other surfactants on DTPC have been precisely investigated.^{7,28,29} Singh et al. have found that DTPC was polymerized to give highly conjugated polymer by addition of saturated short-chain phosphatidylcholines such as 1,2-dinonanoyl-*sn*-glycerol 3-phosphocholine.²⁸ They have proposed that the short-chain saturated phosphatidylcholines match the size of proximal segment between the head group and the diacetylene of DTPC, resulting in the formation of tubular assemblies. In the cases of 2C12S, 2C12N, and 2C14N,

the alkyl segment would mismatch with the proximal segment of DTPC to induce conformational change of polymer backbone of polymerized DTPC. As a result, the additive amphiphiles caused formation of filled aggregates with low F values.

Mechanism of Phase Segregation and Morphological Change. The morphology of **4–5** and **6–8** vesicles depends on the carbon number, n , of 2C n N and 2C n S. The mechanism of the morphological change can be surmised from the fluidity of each of the amphiphiles. The main phase transition temperature (T_c) from the liquid crystalline phase to the solid-analogous phase of DTPC, 2C16S, and 2C12S were reported to be 38.5,¹⁴ 61, and 28 °C,³⁰ respectively. During cooling from 80 to 22.5 °C in the preparation of **4**, the 2C16S components lost fluidity to form a solid domain, but the DTPC still remained fluid up to the T_c of DTPC. This caused the phase segregation of 2C16S from the DTPC component. On the other hand, in the preparation of **5**, DTPC was first crystallized whereas 2C12S remained fluid at the T_c of DTPC. As a result, the fluid 2C12S was blended into the DTPC phase to change the aggregated structure of DTPC molecules from that of pure DTPC. Therefore, T_c values of DTPC and 2C n S determined whether the morphology of the mixed vesicles changed or not. Similarly, the T_c values of 2C16N and 2C14N were determined to be 43 and 35 °C by DSC, respectively (Figure 6). The T_c peak of 2C12N did not appear. It was expected T_c of 2C12N was lower than that of 2C14N. The T_c value of 2C16N, which segregated from the DTPC phase, was larger than that of DTPC, whereas the T_c values of 2C14N and 2C12N, which mixed with the DTPC, were lower than that of DTPC. The dependence of the F values and the morphological change of **6–8** on the carbon number, n , of 2C n N were similar to that of the mixed vesicles of DTPC and 2C n S. Thus, the fluidity of 2C n N and DTPC greatly affected the formation of the mixed vesicles. A similar phase segregation mechanism has been proposed by O'Brien and co-workers for the vesicles of DTPC and nonpolymerizable phosphatidylcholine based on T_c determined by DSC.¹⁶

Conclusion

Phase segregation in vesicles has been previously found in vesicles formed from DTPC and nonpolymerizable phospho-

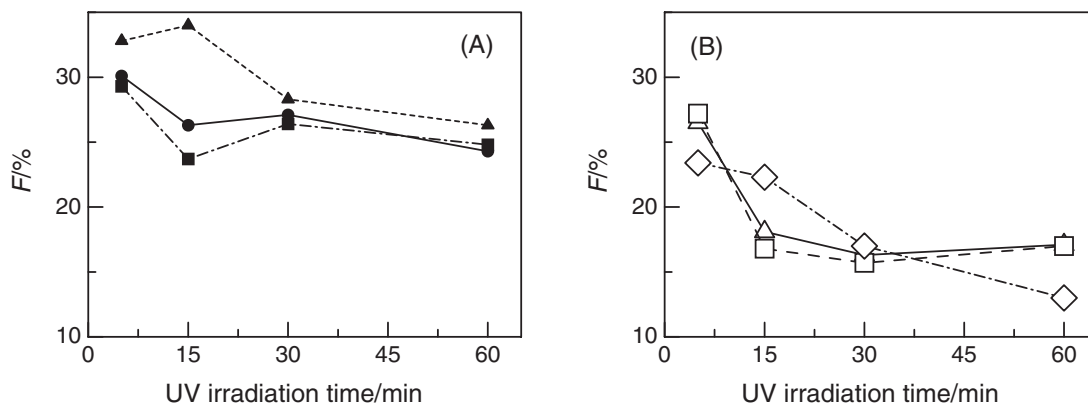


Figure 5. Time course plot of F for (A) the 3 (●), 4 (▲), and 6 (■) and for (B) 5 (△), 7 (□), and 8 (◇) under UV irradiation.

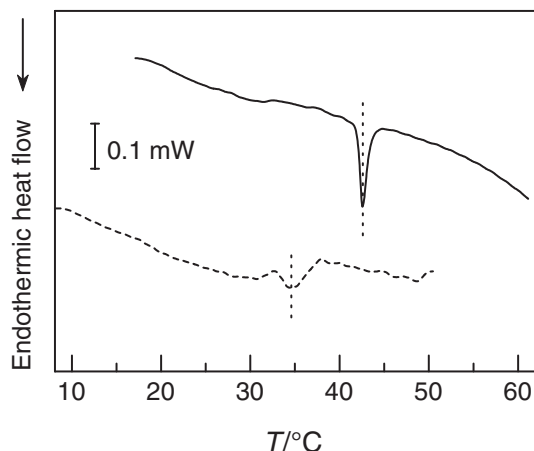


Figure 6. DSC curves of 2C16N solution (solid line) and 2C14N one (broken line).

tidylcholine.^{7,16,31} Here, we have successfully prepared micrometer size GVs of DTPC and nonpolymerizable amphiphiles other than phosphatidylcholine by modified TFH. Thus, the high ability of DTPC to phase-segregate toward a variety of amphiphiles is elucidated.

Based on the analysis of the GVs with CLSM, the morphological change of the mixed GVs of DTPC and nonpolymerizable amphiphiles occurred during the hydration of the films in an aqueous solution by self-assembly. In the TFH method, the addition of nonpolymerizable amphiphiles, which have a different T_c from the main component of DTPC, induced the phase segregation of the polymerized GVs. Moreover, analysis of the visible absorption spectra of the GVs revealed the effects of the additional nonpolymerizable amphiphiles on the polymerization reaction of the DTPC monomers. It is expected that TFH is applicable to development of functionalized GVs.

Supporting Information

Effects of mixing ratio on F values of 6–8 (Figure S1). CLSM images of 6 obtained at the specified z under 488-nm laser excitation (Figure S2). CLSM cross-sectional images of GVs of 2C14N and 2C12N under 543-nm laser excitation (Figure S3). Distribution of the fluorescence intensity along a line on a cross-sectional CLSM images of 7 under 488-nm laser

excitation (Figure S4). CLSM images of 7 and 8 obtained at the specified z under 488-nm laser excitation (Figure S5). This material is available free of charge on the web at <http://www.csj.jp/journals/bcsj/>.

References

- 1 K. Ariga, J. P. Hill, M. V. Lee, A. Vinu, R. Charvet, S. Acharya, *Sci. Technol. Adv. Mater.* **2008**, 9, 014109.
- 2 J.-H. Ryu, D.-J. Hong, M. Lee, *Chem. Commun.* **2008**, 1043.
- 3 V. P. Torchilin, *Nat. Rev. Drug Discovery* **2005**, 4, 145.
- 4 H. Ringsdorf, B. Schlarb, J. Venzmer, *Angew. Chem., Int. Ed. Engl.* **1988**, 27, 113.
- 5 A. Mueller, D. F. O'Brien, *Chem. Rev.* **2002**, 102, 727.
- 6 S. Alonso-Romanowski, N. S. Chiamoni, V. S. Liroy, R. A. Gargini, L. I. Viera, M. C. Taira, *Chem. Phys. Lipids* **2003**, 122, 191.
- 7 A. Yavlovich, A. Singh, S. Tarasov, J. Capala, R. Blumenthal, A. Puri, *J. Therm. Anal. Calorim.* **2009**, 98, 97.
- 8 C. Guo, S. Liu, C. Jiang, W. Li, Z. Dai, H. Fritz, X. Wu, *Langmuir* **2009**, 25, 13114.
- 9 M. A. Reppy, B. A. Pindzola, *Chem. Commun.* **2007**, 4317.
- 10 Y. K. Jung, H. G. Park, J.-M. Kim, *Biosens. Bioelectron.* **2006**, 21, 1536.
- 11 K. Suzuki, T. Toyota, K. Takakura, T. Sugawara, *Chem. Lett.* **2009**, 38, 1010.
- 12 W. H. Binder, V. Barragan, F. M. Menger, *Angew. Chem., Int. Ed.* **2003**, 42, 5802.
- 13 J. Koriach, P. Schwill, W. W. Webb, G. W. Feigenson, *Proc. Natl. Acad. Sci. U.S.A.* **1999**, 96, 8461.
- 14 D. S. Johnston, S. Sanghera, M. Pons, D. Chapman, *Biochim. Biophys. Acta, Biomembr.* **1980**, 602, 57.
- 15 D. F. O'Brien, T. H. Whitesides, R. T. Klingbiel, *J. Polym. Sci., Polym. Lett. Ed.* **1981**, 19, 95.
- 16 E. Lopez, D. F. O'Brien, T. H. Whitesides, *Biochim. Biophys. Acta, Biomembr.* **1982**, 693, 437.
- 17 T. Okazaki, T. Inaba, Y. Tatsu, R. Tero, T. Urisu, K. Morigaki, *Langmuir* **2009**, 25, 345.
- 18 J. Olmsted, III, M. Strand, *J. Phys. Chem.* **1983**, 87, 4790.
- 19 T. Kobayashi, M. Yasuda, S. Okada, H. Matsuda, H. Nakanishi, *Chem. Phys. Lett.* **1997**, 267, 472.
- 20 T. Kunitake, Y. Okahata, *Bull. Chem. Soc. Jpn.* **1978**, 51, 1877.
- 21 P. Yager, P. E. Schoen, *Mol. Cryst. Liq. Cryst.* **1984**, 106,

371.

22 J. H. Georger, A. Singh, R. R. Price, J. M. Schnur, P. Yager, P. E. Schoen, *J. Am. Chem. Soc.* **1987**, *109*, 6169.

23 G. Wegner, *Pure Appl. Chem.* **1977**, *49*, 443.

24 R. H. Baughman, R. R. Chance, *J. Polym. Sci., Polym. Phys. Ed.* **1976**, *14*, 2037.

25 R. R. Chance, *Macromolecules* **1980**, *13*, 396.

26 M. F. Rubner, D. J. Sandman, C. Velazquez, *Macromolecules* **1987**, *20*, 1296.

27 C. Kollmar, H. Sixl, *J. Chem. Phys.* **1988**, *88*, 1343.

28 D. G. Rhodes, A. Singh, *Chem. Phys. Lipids* **1991**, *59*, 215.

29 B. M. Peek, J. H. Callahan, K. Namboodiri, A. Singh, B. P. Gaber, *Macromolecules* **1994**, *27*, 292.

30 Y. Okahata, R. Ando, T. Kunitake, *Ber. Bunsen-Ges. Phys. Chem.* **1981**, *85*, 789.

31 E. Sackmann, P. Eggl, C. Fahn, H. Bader, H. Ringsdorf, M. Schollmeier, *Ber. Bunsen-Ges. Phys. Chem.* **1985**, *89*, 1198.